Applied Surface Science 234, pp.387-394(2004)

Effects of nitrogen deficiency on electronic properties of AlGaN surfaces subjected to thermal and plasma processes

Tamotsu Hashizume[a] and Hideki Hasegawa

Research Center for Integrated Quantum Electronics (RCIQE),

Hokkaido University, Sapporo, 060-8628, Japan

Abstract

Effects of device processing on chemical and electronic properties of AlGaN surfaces were investigated. The X-ray photoelectron spectroscopy analysis showed serious deterioration such as stoichiometry disorder and nitrogen deficiency (N deficiency) at the AlGaN surfaces processed by high-temperature annealing, H_2-plasma cleaning, dry etching in $CH_4/H_2/Ar$ plasma and deposition of SiO_2. This resulted in high density of surface states at the processed AlGaN surface. Furthermore, the N deficiency introduced a localized deep donor level related to N vacancy (V_N) at AlGaN surfaces. Such electronic states governed by a V_N- related deep donor and surface state continuum can cause strong Fermi level pinning at the AlGaN surface, reduction of the barrier height and excess leakage currents at the AlGaN Schottky interface and serious drain current collapse in AlGaN/GaN heterostructure field effect transistors. The SiN_x- or Al_2O_3- based passivation scheme with a combination of a remote N_2-plasma treatment was found to be effective in suppressing formation of V_N- related surface defects at AlGaN surfaces.

[a] E-mail: hashi@rciqe.hokudai.ac.jp

1. Introduction

The fabrication process of semiconductor devices involves various kinds of surface treatments and junction formation steps under high-temperature and/or high-processing energy conditions, which may disorder chemical composition and introduce defects on semiconductor surfaces. Although significant progress has been achieved in the GaN-based high-power/high-frequency electronic devices, additional works are required to solve surface-related problems. In particular, the so-called current collapse effects not only degrade microwave-output performance but also impede reliable operation of the GaN-based power devices [1-5]. To understand and control instability issues in AlGaN/GaN heterostructure field effect transistors (HFETs), it is important to clarify the properties of process-induced defects on AlGaN surfaces. However, experimental confirmation on the electronic states of such "surface defects" has largely been lacking.

The present paper reports effects of device processing on chemical and electronic properties of AlGaN surfaces, especially focusing on nitrogen deficiency caused by high-temperature annealing, plasma cleaning, plasma etching and plasma-assisted deposition processes. It is shown that a nitrogen-vacancy-related near-surface trap plays an important role in electronic states of AlGaN surfaces and operation stability of AlGaN/GaN HFETs.

2. Experiment

2.1 Samples

The $Al_{0.25}Ga_{0.75}N$/GaN heterostructure sample grown on sapphire substrate by metal organic vapor phase epitaxy (MOVPE) was used in this study. The AlGaN barrier consists of an undoped capping layer (5 nm), a Si-doped layer (15 nm, 4×10^{18} cm^{-3}) and an undoped spacer layer (5 nm). Typical values of electron mobility and sheet carrier concentration of the heterostructure samples at room temperature (RT) is 900 cm^2/Vs and 1.1×10^{13} cm^{-2}, respectively. We also prepared Si-doped n-type $Al_{0.20}Ga_{0.80}N$ layer (0.5 μm) grown by MOVPE for metal-insulator-semiconductor (MIS) and Schottky-junction structures. The mobility and carrier concentration at RT were 100 cm^2/Vs and $5 \times 10^{17} cm^{-3}$, respectively. The dislocation density of AlGaN layers ranged from 1×10^9 - 4×10^9 cm^{-2}.

2.2 Surface processes

To reduce natural oxide, all the AlGaN surfaces were initially treated in NH_4OH solution at 50 °C for 10 min [6, 7]. We used this surface as a reference. Then the samples were processed by thermal annealing, plasma cleaning, dry etching and deposition of SiO_2 and SiN_x films. The annealing was performed in N_2 at 900 °C for 1 min with and without a SiN_x cap. The electron-cyclotron-resonance (ECR) excited H_2 plasma with a microwave power of 50 W was used as a dry plasma-cleaning process for AlGaN surfaces at 300 °C. The ECR-assisted reactive ion-beam etching (ECR-RIBE) of the AlGaN surfaces was carried out at RT using a $CH_4/H_2/Ar$ gas system [8]. The deposition of SiO_2 and SiN_x was performed at 280 °C by ECR-assisted chemical vapor deposition, using SiH_4 and N_2O as precursors for SiO_2, and SiH_4 and N_2 for SiN_x, respectively. The thickness of the deposited films ranged from 2 to 70 nm.

3. Results and Discussion

3.1 XPS characterization of processed AlGaN surfaces

Figure 1 shows X-ray photoelectron spectroscopy (XPS) core-level spectra of the $Al_{0.25}Ga_{0.75}N$/GaN heterostructure surfaces after the annealing at 900 °C for 1min in N_2 flow. A monochromated Al Kα x-ray source ($h\nu = 1486.6$ eV) was used for the XPS measurements. The present annealing condition is typical for an alloying process for formation of ohmic contacts on AlGaN surfaces. As shown in Fig. 1 (a), the high-temperature anneal produced large amounts of oxide and metal elements in the Al2*p* spectrum. A similar feature was observed in the Ga3*d* core level. This means that a residual O_2 or H_2O in N_2 atmosphere can cause oxidation reaction at the AlGaN surface under the high-temperature condition. From the N1*s* spectrum, a serious N deficiency was seen at the annealed AlGaN surface, as shown in Fig. 1 (c). In addition, the peak corresponding to the N-O bond [9] was detected at the annealed surface. Such degradation of chemical properties was also observed at

the AlGaN surfaces after dry etching in $CH_4/H_2/Ar$ plasma, as shown in **Fig.2**. This process left large amounts of metal clusters on the AlGaN surfaces, resulting in pronounced disorder in the surface stoichiometry.

Table I summarizes the XPS analysis on the AlGaN/GaN heterostructure sample surfaces after various treatments. We firstly deconvoluted the measured XPS spectra into some chemical bonding components, as shown in Figs.1 and 2. The Al2p and Ga3d spectra were deconvoluted into the AlGaN bonds, the metallic bonds and oxide bonds, while the N1s peak was separated to the AlGaN bond, Ga AES peaks and additional NH_x or NO_x peaks. The composition and V/III ratio were then calculated from the integrated intensities of the deconvoluted XPS components taking account the sensitivity factors.

As mentioned above, the high-temperature anneal caused highly non-stoichiometric surface (V/III ratio of 0.87). The apparent Al composition became much higher than that before annealing. This seems to be due to formation of large amounts of metallic Al cluster and Al oxide, as shown in Fig. 1 (a). As seen in Table I, the degradation of chemical properties was also observed on the AlGaN surfaces after H_2-plasma, RIBE and SiO_2-deposition processes (samples C-E). A model for possible surface reactions during these processes is shown in **Fig.3**. During high-temperature annealing, residual impurities such as O_2 and/or H_2O in N_2 can cause oxidation reaction at the AlGaN surface. The N atoms dissociated from Al-N and Ga-N bonds due to the oxidation could react each other or with O atoms to form volatile molecules such as N_2 or NO_x. This led to the preferential loss of N atoms from the AlGaN surface, leaving a residue of oxides and metal clusters, as shown in Fig.3 (a). The increase of Al composition after the high-temperature annealing indicated that such surface processes also caused a Ga evaporation.

After the deposition of the SiO_2 film, we detected an enhancement of the oxide components on the AlGaN surface. In the initial stage of the deposition process, O-related radicals generated in the N_2O plasma may react with AlGaN surface, resulting in loss of N atoms and surface process partly similar to that in the high-temperature annealing.

During the H_2-plasma treatment, highly active H radicals can react with the AlGaN surface to form volatile NH_x products, as schematically shown in Fig. 3 (b), even at low temperature around 300 ^oC. This process left the III-metal droplets or clusters and the N depletion at the topmost AlGaN surface [10, 11]. For the RIBE process using $CH_4/H_2/Ar$ plasma, a similar surface reaction can occur at AlGaN surfaces, producing a heavily metal-rich AlGaN surface [8]. This also led to the pronounced deficiency of N atoms (V/III ratio of 0.56).

3.2 Electronic states of processed AlGaN surfaces

To investigate the effects of N deficiency on electronic properties of AlGaN surface, the C-V and I-V measurements were employed to the processed surfaces using metal-insulator-semiconductor (MIS) and Schottky-junction structures.

Figure 4 shows the interface state density distributions (D_{it}) of the $SiN_x/n\text{-}Al_{0.2}Ga_{0.8}N$ structures determined by applying the Terman method to the measured C-V data at room temperature. The SiN_x film was deposited on the processed AlGaN. The measurement frequency was 100 kHz. The sample treated only in NH_4OH solution (reference sample) showed a normal continuous D_{it} distribution [6, 10]. On the other hand, a localized surface level was found at around E_C-0.4 eV for the sample with the high-temperature annealed AlGaN surface, as shown in Fig.4. Such a discrete level was also detected in the H_2-plasma-processed and RIBE-processed samples where serious N deficiency was found. These results indicated that the N deficiency seems to introduce a nitrogen-vacancy (V_N) -related gap level at the processed AlGaN surfaces. Neugebauer and Van de Walle [12], and Boguslawski et al. [13] predicted that a simple V_N defect creates donor levels in the conduction band, acting as a resonant or shallow donor levels in GaN. On the other hand, a possibility of an s-like discrete deep level within bandgap was proposed for a V_N defect in GaN and AlGaN by Yamaguchi and Junnarkar [14]

Next, we have calculated the pinning positions of surface Fermi levels (E_{FS}) at the processed AlGaN surfaces based on the experimentally obtained surface state distributions shown in Fig.4. For simply formulating the distribution, we used a surface state model which consists of a U-shaped surface state continuum and a discrete donor level, as shown in **Fig.5 (a)**. For the U-shaped

distribution, the following formula was used in accordance with the disorder-induced gap state (DIGS) model [15].

$$D_{SS}(E) = D_{SS\,\min} \exp(|E - E_{CNL}| / E_0)^n \qquad (1)$$

where D_{SSmin} is the minimum surface state density and E_{CNL} is the charge neutrality level. E_{CNL} acts as a branch point of surface or interface states since they can be related to the conduction band or the valence band. This represents that the state continuum distributed in energy above E_{CNL}, which has conduction-band character, is acceptor-like charging state, while the one below E_{CNL} splitting off from the valence band has donor-like charging state [16]. E_O and n are the parameters related to distribution shape of a state continuum. The position of E_{CNL} was set at the midgap of AlGaN. For the discrete near-surface donor level, we employed a donor-type Gaussian peak [12-14] at E_C-0.4 eV with a thermal distribution of 3kT (k: Boltzmann constant, T: absolute temperature). The Al composition was assumed to be 0.3 because it is often used for AlGaN/GaN HFET structures.

The position of E_{FS} (= E_C-E_F at the surface) was calculated applying the charge neutrality condition to the AlGaN surface.

$$\int_{E_{CNL}}^{E_{FS}} D_{SS}(E)dE = D_{SS}^{-} = D_{VN}^{+} + D_{dep}^{+} \qquad (2)$$

where D_{SS}^-, D_{VN}^+ and D_{dep}^+ are the ionized acceptor-like surface states, ionized V_N-related level and ionized shallow donors in depletion region of the AlGaN surface. The calculated E_{FS} position is plotted as a function of the minimum value of surface state continuum, D_{ssmin}, in Fig. 5 (b). The band bending at the $Al_{0.3}Ga_{0.7}N$ surface becomes stronger with the density of state continuum. In general, semiconductor surfaces processed with high energy show non-stoichiometric and highly-disordered character, resulting in formation of high-density surface states. This can lead to the strong band bending at the surfaces. The E_{FS} values ranging from 1.3 eV to 1.7 eV have often been reported for $Al_xGa_{1-x}N$ surface (x: 0.24 - 0.41) [17-19]. From the calculated results shown in Fig. 5 (b), it is expected that surface states with densities higher than 1 x 10^{12} cm^{-2} eV^{-1} are formed on the processed AlGaN surfaces, thereby causing the firm Fermi level pinning.

When a V_N-related discrete donor level is introduced at the surface, the band bending is apparently reduced, as shown in Fig. 5 (b), assuming that the density of state continuum remains unchanged. An extremely high density of the V_N-related donor, in particular, can lower the E_{FS} position below 1.0 eV. This may be the case for molecular-beam-epitaxy (MBE) grown GaN surfaces [20] where the Ga-rich condition is likely due to the limitation of nitrogen supply via rf-plasma-excited source and highly non-equilibrium growth condition for MBE [21]. For practical processed surface, however, the N deficiency is accompanied by serious surface disorder described in the previous section. This may also cause an increase in density of the surface state continuum. In such a case, there is a possibility that the E_{FS} position almost remains unchanged even if the V_N-related defect was created at the processed surfaces.

The surface electronic states obtained here can cause various kinds of operation instabilities in AlGaN/GaN HFETs due to trapping and detrapping of electrons by surface states. In fact, Hasegawa et al. [22] have very recently reported that the electronic states consisting of a U-shaped state continuum and a V_N-related defect level were responsible for drain current collapse in AlGaN/GaN HFETs. According to this model, such surface states could be filled with high-energy electrons injected from the channel during on-state operation with a large drain voltage. This could form a "virtual gate" at the free AlGaN surface near drain edge and partially deplete the two-dimensional electron gas at the AlGaN/GaN interface. In the off-state operation, the strong gate stress may induce electron injection into surface states near gate edge between gate and drain, also causing similar virtual gating effects on the AlGaN surface. Thus, the drain current collapse was induced under both drain stress and gate stress [1-5, 22].

The effects of V_N-related defect level on Schottky properties of AlGaN were investigated. **Figure 6** shows typical I-V characteristics of Ni/n-$Al_{0.20}Ga_{0.80}N$ Schottky interfaces with and without the H_2-plasma treatment. The sample without the H_2-plasma treatment showed the I-V curve similar to

the published data [23-25]. On the other hand, the pronounced reduction of barrier height, φ_B, was observed for the sample having the AlGaN surface exposed to the H_2 plasma. The RIBE process resulted in similar reduction of φ_B. The high-density V_N-related donors induced during the plasma processes seem to be responsible for the serious thinning of potential barrier at the Schottky interface. In that case, electron transport across the interface is not governed by normal thermionic emission but by thermionic field emission [26], leading to significant reduction of the effective potential barrier against electrons. Such reduction of barrier heights were reported on the GaN and AlGaN surfaces processed by reactive ion etching (RIE) [23, 27] and inductively coupled plasma (ICP)-assisted etching [28, 29]. It is expected that high-density V_N-related donor levels are introduced at the surfaces during those etching processes. In addition, Hasegawa et al. [22] recently pointed out that introduction of high-density V_N-related donor level caused pronounced thinning of Schottky barrier, resulting in serious excess gate leakage currents in the AlGaN/GaN HFETs due to thermionic field emission transport [26].

3.3 Surface passivation processes for AlGaN surfaces

For reliability improvement of GaN-based electron devices such as AlGaN/GaN HFETs, it is inevitable to establish a suitable passivation structure for AlGaN surfaces especially for suppressing N deficiency.

Firstly, we employed a surface treatment process using N_2 plasma for AlGaN. The process utilized a remote ECR plasma where electrons and ions move with the same diffusion coefficient, i.e., the so-called ambipolar diffusion [30]. This means that a nearly neutrality condition can be maintained in the plasma stream. In addition, the ECR microwave discharges can be produced without large potentials. Thus, it is expected that a self-biasing effect is rather weak in the ECR plasma processes. In fact, Matsuoka and Ono [31] reported the self-biasing voltage less than - 40 V in the gas pressure range from 1×10^{-2} Pa to 1×10^{-1} Pa. This fact as well as low ion energies of 10 to several tens of eV in the ECR plasma [31, 32] can suppress an ion-bombardment (sputtering) effect on the material surfaces.

Figure 7 shows the XPS O1s and C1s spectra of $Al_{0.25}Ga_{0.75}N$ surface before and after the ECR N_2-plasma treatment with a relatively low microwave power of 50 W. The process time and temperature was 1 min and 280 ^oC, respectively. Significant reduction of O1s and C1s peaks was observed at the AlGaN surface after the N_2-plasma treatment, indicating the process is effective in removing natural oxide from AlGaN surfaces. The Al composition and V/III ratio was maintained even after the N_2-plasma process. Furthermore, the band bending was reduced at the N_2-plasma-treated GaN surfaces [6]. These results indicate that the ECR N_2-plasma treatment seems to partially recover or terminate V_N-related defects, leading to the reduction of densities of surface states on GaN and AlGaN.

Next we investigated a surface passivation scheme utilizing the ECR N_2-plasma treatment and deposition of SiN_x film. The capacitance-voltage analysis showed relatively low interface state density of 1×10^{11} $cm^{-2}eV^{-1}$ or less at the SiN_x/GaN interface [6, 33]. This seems to be main reason that the SiN_x-based surface passivation effectively suppress current collapse in GaN MESFETs [34] and AlGaN/GaN HFETs [4, 5, 35-38]. From XPS analysis on the annealed AlGaN surface after removing a SiN_x passivation layer, we found that the SiN_x passivation was also effective in suppressing surface disorder of AlGaN during high-temperature annealing. In contrast to the result shown in Fig.1, no deterioration in chemical configuration was observed at the SiN_x-passivated surface even after the high-temperature annealing. In addition, the peak positions and line widths of the core-level spectra remained unchanged. Thus the SiN_x film can act as a protective layer against chemical reaction at AlGaN surfaces during the annealing process.

The SiN_x film has also been used as a gate insulator for AlGaN/GaN HFETs [5, 39]. However, it can be argued that its bandgap ($E_G \sim 5$ eV) and dielectric constant ($\varepsilon \sim 7$) are not suitable for utilization as a gate barrier to $Al_xGa_{1-x}N$ (eg., $E_G \sim 4.1$ eV and $\varepsilon \sim 9$ for $x = 0.3$). In fact, we have very recently pointed out that there was a Fowler-Nordheim leakage problem at the $SiN_x/Al_{0.3}Ga_{0.7}N$ interface due to a low value of conduction band offset [11]. As an alternative gate dielectric, we proposed the use of Al_2O_3 for AlGaN/GaN HFET since it has a wide bandgap (> 7 eV), a high

dielectric constant (~ 9) and a high breakdown field (> 15 MV/cm). The fabricated Al_2O_3 insulated gate HFET showed an excellent gate control of currents with low gate leakage characteristics. In addition, the Al_2O_3-based surface passivation scheme including an N_2-plasma surface treatment achieved the drastic suppression of current collapse in AlGaN/GaN HFETs [11, 40].

4. Summary

The effects of device processing on chemical and electronic properties of AlGaN surfaces were investigated by XPS, C-V and I-V methods. Serious stoichiometry disorder and N deficiency were found at the AlGaN surfaces processed by high-temperature annealing, H_2-plasma cleaning, dry etching in $CH_4/H_2/Ar$ plasma and deposition of SiO_2. The N deficiency could introduce a localized deep donor level related to N vacancy (V_N) at AlGaN surfaces. The electronic states governed by a V_N-related deep donor and surface state continuum can cause reduction of the barrier height and excess leakage currents at the AlGaN Schottky interface and serious drain current collapse in AlGaN/GaN heterostructure field effect transistors. The results obtained indicate that it becomes a key to control V_N-related defects for reliability improvement of GaN-based electronic devices. The SiN_x- or Al_2O_3-based passivation scheme with a combination of a remote N_2-plasma treatment is promising for suppressing formation of V_N-related surface defects as well as reducing surface state continuum at AlGaN surfaces.

Acknowledgements

This work was partly supported by a grant-in-aid for Scientific Research (B) (#14350155) from Ministry of Education, Culture, Sports, Science and Technology, and by a grant from the Support Center for Advanced Telecommunications Technology Research (SCAT).

References

[1] C. Nguyen, N.X. Nguyen,and D.E. Grider, Electron. Lett. **35**, 1380(1999).
[2] K. Kunihiro, K. Kasahara, Y. Takahashi, and Y. Ohno, Jpn. J. Appl. Phys. **39**, 2431(2000).
[3] S. Binari, K. Ikosssi, J. Roussos, W. Kruppa, D. Park, H. Dietrich, D. Koleske, A. Wickenden, and R. Henry, IEEE Trans. Electron Devices **48**, 465(2001).
[4] T. Kikkawa, M. Nagahara, N. Okamoto, Y. Tateno, Y. Yamaguchi, N. Hara, K. Joshin, and P.M. Asbeck, 2001 IEDM Technical Digest, p.585, (2001).
[5] T. Mizutani, Y. Ohno, M. Akita, S. Kishimoto, and K. Maezawa, phys. stat. sol. (a) **194**, 447(2002).
[6] T. Hashizume, S. Ootomo, S. Oyama, M. Konishi, and H. Hasegawa, J. Vac. Sci. Technol. B **19**, 1675(2001).
[7] T. Hashizume, S. Ootomo, R. Nakasaki, S. Oyama, M. Kihara, Appl. Phys. Lett., **76**, 2880(2000).
[8] Z. Jin, T. Hashizume, and H. Hasegawa, Appl. Sur. Sci. **190**, 361(2002).
[9] A. Baraldi et al, J. Electron Spectrosc. Relat. Phenom. **76**, 145(1995).
[10] T. Hashizume and R. Nakasaki, Appl. Phys. Lett. **80**, 4564(2002).
[11] T. Hashizume, S. Ootomo, T. Inagaki, and H. Hasegawa, J. Vac. Sci. Technol. B **21**, 1828(2003).
[12] J. Neugebauer and C. G. Van de Walle, Phys. Rev. B **50**, 8067(1994).
[13] P. Boguslawski, E.L. Briggs, and J. Bernholc, Phys. Rev. B **51**, 17255(1995).
[14] E. Yamaguchi, and M. R. Junnarkar, J. Crystal Growth **189/190**, 570(1998).
[15] H. Hasegawa and H. Ohno, J. Vac. Sci. Technol. B **4**, 1130(1986).
[16] H. Luth, *"Surfaces and Interfaces of Solids"*, 2nd. Ed., Chapter 6, Splinger-Verlag, Berlin, 1993.
[17] H.W. Jiang, C.M. Jeon, K.H. Kim, J.K. Kim, S.B. Bae, J.H. Lee, J.W. Choi, and J.L. Lee, Appl. Phys. Lett. **81**, 1249(2002).
[18] A. Rizzi and H. Luth, Appl. Phys. A **75**, 69(2002).
[19] S. Heikman, S. Keller, Y. Wu, J.S. Speck, S.P. DenBaars, and .K. Mishra, J. Appl. Phys. **93**, 10114(2003).
[20] M. Kocan, A. Rizzi, H. Luth, S. Keller,and U.K. Mishra, phys. stat. sol. (b) **234**, 773 (2002).
[21] O. Ambacher, M.S. Brandt, R. Dimitrov, T. Metzger, M. Stutzmann, R.A. Fischer, A. Miehr, A. Bergmaier and G. Dollinger, J. Vac. Sci. Technol. B **14**, 3532(1996).
[22] H. Hasegawa, T. Inagaki, S. ootomo, and T. Hashizume, J. Vac. Sci. Technol. B **21**, 1844(2003).
[23] E. Monroy et al., J. Appl. Phys. **88**, 2081(2000).
[24] E.D. Readinger, B.P. Luther, S. E Mohney, and E.L. Piner, J. Appl. Phys. **89**, 7983(2001).
[25] J. Kuzmik, P. Javorka, M. Marso, and P. Kordos, Semicond. Sci. Technol. **17**, L76(2002).
[26] F. A. Padovani, and R. Stratton, Solid State Electron. **9**, 695(1966).
[27] A.T. Ping, A.C. Schmitz, I. Adesida, M.A. Khan, Q. Chen, and J.W. Yang, J. Electron. Mat. **26**, 266(1997).
[28] A.P. Zhang et al., J. Electrochem. Soc. **147**, 719(2000).
[29] K. J. Choi, H. W. Jang, and J-L. Lee, Appl. Phys. Lett, **82**, 1233(2003).
[30] J. Asmussen, J. Vac. Sci. Technol. A **7**, 883(1989)
[31] M. Matsuoka and K. Ono, J. Vac. Sci. Technol. A **6**, 25(1988).
[32] G. W. Gibson, Jr., H. H. Sawin, I. Tepermeister, D. E. Ibbotson, and J. T. C. Lee, J. Vac. Sci. Technol. B **12**, 2333(1994).
[33] R. Nakasaki, T. Hashizume and H. Hasegawa, Physica E **7**, 953(2000).
[34] A. Jimenez, D. Buttari, D. Jena, R. Coffie, S. Heikman, N. Q. Zhang, L. Shen, E. Calleja, E. Munoz, J. Speck, and U. K. Mishra, IEEE Electron Device Lett. **23**, 306(2002).
[35] R. Vetury, N.Q. Zhang, S. Keller and U.K. Mishra, IEEE Trans. Electron Devices **48**, 560(2001).
[36] C. Koley, V. Tilak, L.F. Eastman, and M.G. Spencer, IEEE Trans. Electron Devices **50**, 886(2003).
[37] J.A. Mittereder, S.C. Binari, P.B. Klein, J.A. Roussos, D.S. Katzer, D.F. Storm, D.D. Koleske, A.E. Wickenden, and R.L. Henry, Appl. Phys. Lett. **83**, 1650(2003).
[38] J. Bernat, P. Javorka, A. Fox, M. Marso, H. Luth, and P. Kordos, Solid State Electronics, **47**, 2097(2003).
[39] X. Hu, A. Koudymov, G. Simin, J. Yang, M. A. Khan, A. Tarakji, M. S. Shur and R. Gaska, Appl. Phys. Lett. **79**, 2832 (2001).

[40] T. Hashizume, S. Ootomo and H. Hasegawa, Appl. Phys. Lett. **83**, 2952(2003).

Table caption

Table I Summary of XPS analysis on the processed $Al_{0.25}Ga_{0.75}N$/GaN heterostructure surfaces.

Figure captions

Fig.1 XPS core-level spectra of $Al_{0.25}Ga_{0.75}N$ surface before and after the annealing in N_2 at 900 ^oC for 1 min.

Fig.2 XPS Al2p and Ga3d spectra of $Al_{0.25}Ga_{0.75}N$ surface after the RIBE process in $CH_4/H_2/Ar$ plasma.

Fig.3 schematic illustration of possible surface reactions at the AlGaN surface for (a) the high-temperature annealing process and (b) the H_2-plasma process.

Fig.4 Interface state density distributions (D_{it}) of SiN_x/n-$Al_{0.20}Ga_{0.80}N$ structures. For the annealed sample, the SiN_x film was deposited on the AlGaN surface after the annealing.

Fig.5 (a) An electronic state model and (b) calculated surface Fermi level positions at the $Al_{0.3}Ga_{0.7}N$ surface.

Fig.6 I-V characteristics of the Ni/n-$Al_{0.20}Ga_{0.80}N$ junction with and without the H_2 plasma treatment at 300 ^oC for 1 min.

Fig.7 XPS O1s and C1s spectra of $Al_{0.25}Ga_{0.75}N$ surface before and after the ECR-N_2 plasma treatment at 280 ^oC for 1 min.

Table I Summary of XPS analysis on the processed $Al_{0.25}Ga_{0.75}N$/GaN heterostructure surfaces.

sample	process	Al composition	V/III ratio	Al-oxide ratio in Al2*p* (%)	Ga-oxide ratio in Ga3*d* (%)
A (reference)	NH_4OH	0.25	1.00	6.3	3.4
B	annealed at 900 ^{o}C (w/o SiN_x)	0.38	0.87	40.3	18.7
C	H_2 plasma 300 ^{o}C	0.33	0.81	1.9	1.4
D	RIBE in $CH_4/H_2/Ar$	0.41	0.56	1.3	1.1
E	SiO_2 deposition	0.28	0.91	10.3	8.9

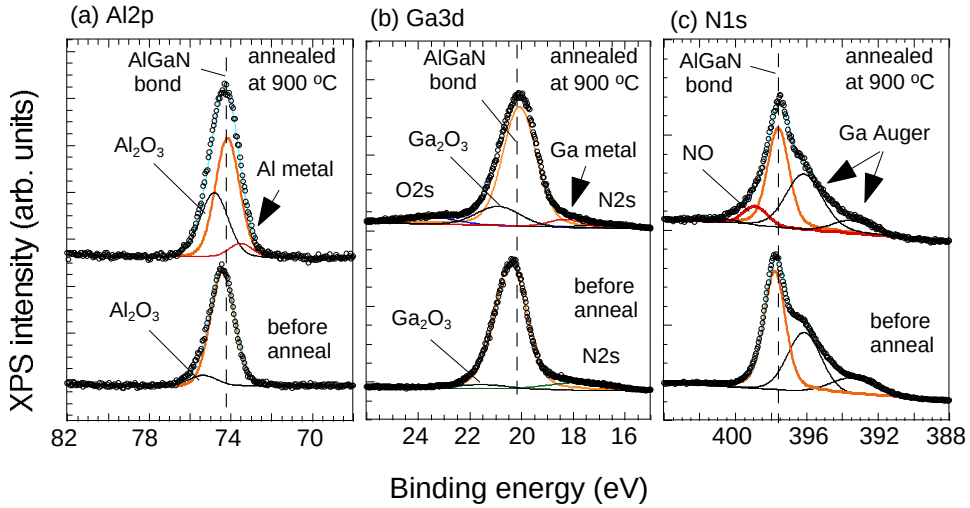

Fig.1 XPS core-level spectra of $Al_{0.25}Ga_{0.75}N$ surface before and after the annealing in N_2 at 900 ^{o}C for 1 min.

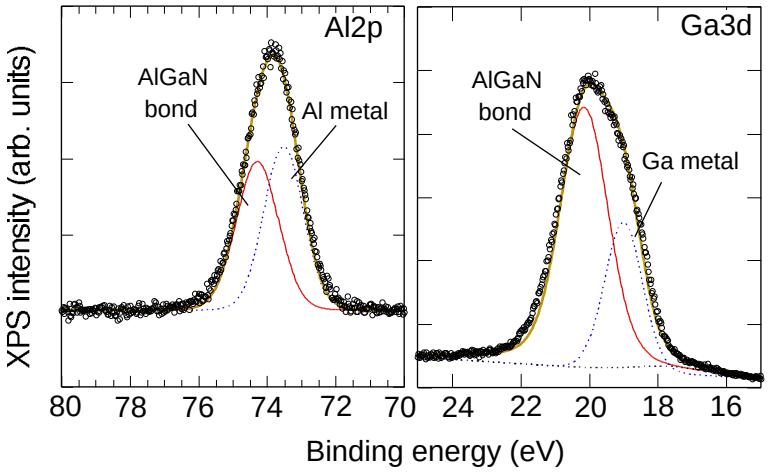

Fig.2 XPS Al2p and Ga3d spectra of $Al_{0.25}Ga_{0.75}N$ surface after the RIBE process in $CH_4/H_2/Ar$ plasma.

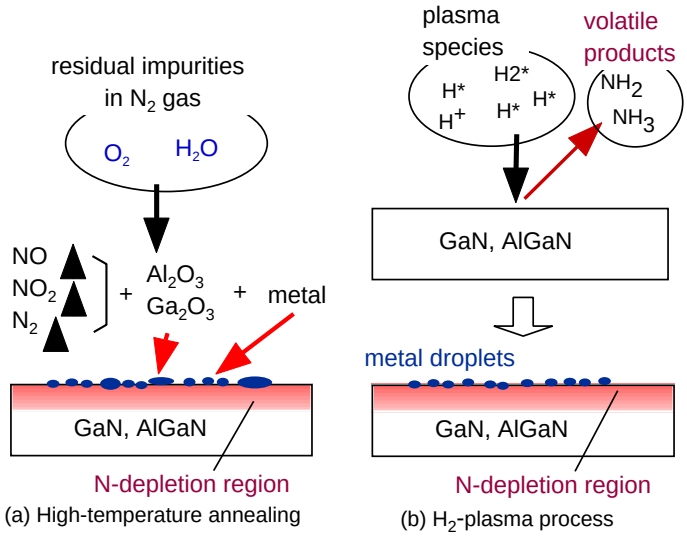

Fig.3 schematic illustration of possible surface reactions at the AlGaN surface for (a) the high-temperature annealing process and (b) the H2-plasma process.

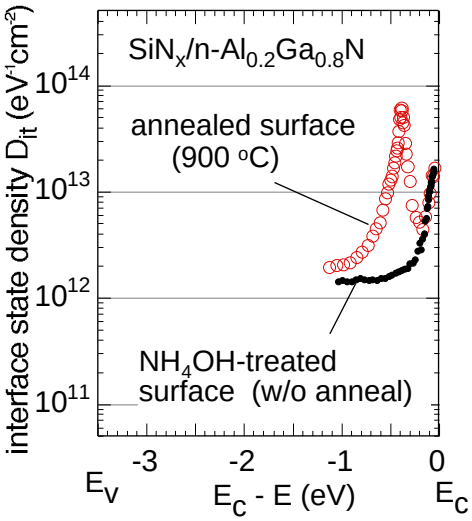

Fig.4 Interface state density distributions (D_{it}) of SiNx/n-$Al_{0.20}Ga_{0.80}N$ structures. For the annealed sample, the SiN_x film was deposited on the AlGaN surface after the annealing.

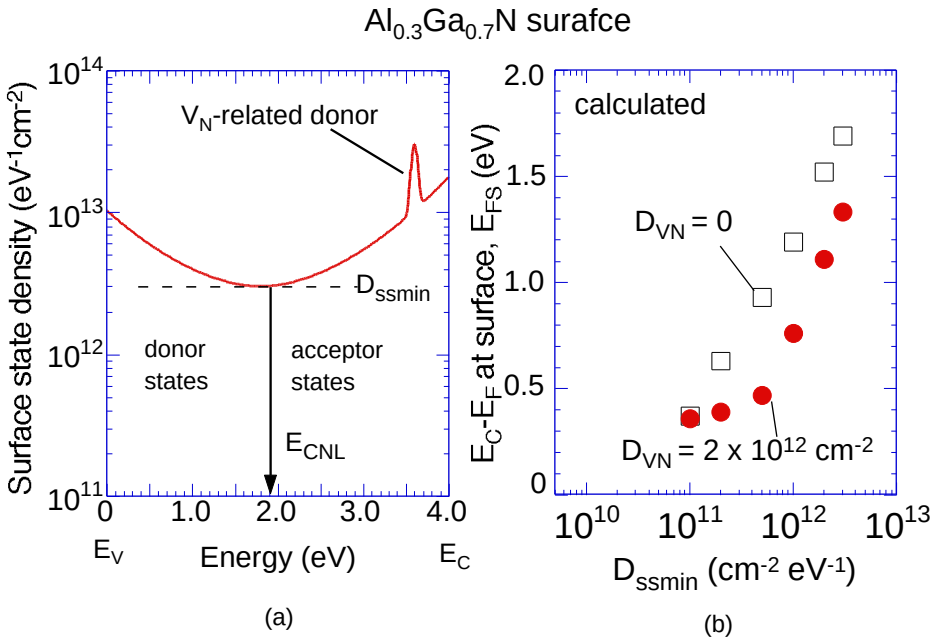

Fig.5 (a) An electronic state model and (b) calculated surface Fermi level positions at the $Al_{0.3}Ga_{0.7}N$ surface.

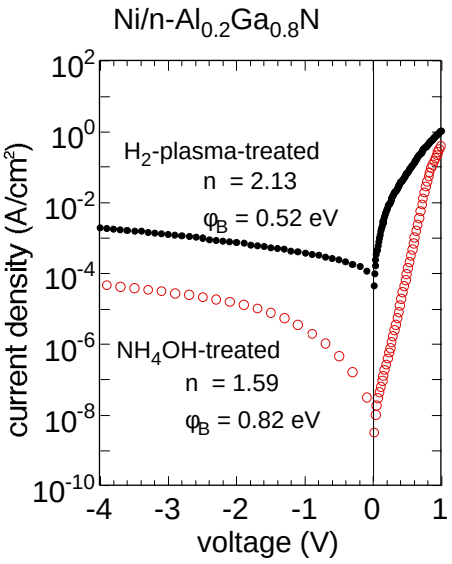

Fig.6 I-V characteristics of the Ni/n-$Al_{0.20}Ga_{0.80}N$ junction with and without the H_2 plasma treatment at 300 ^oC for 1 min.

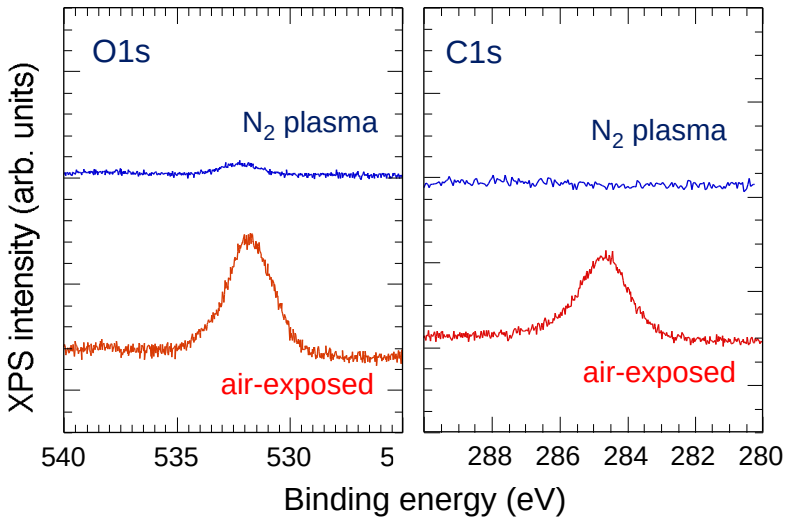

Fig.7 XPS O1s and C1s spectra of $Al_{0.25}Ga_{0.75}N$ surface before and after the ECR-N_2 plasma treatment at 280 ^oC for 1 min.